Applied Surface Science 459 (2018) 201–207

Contents lists available at ScienceDirect

Applied Surface Science

journal homepage: www.elsevier.com/locate/apsusc

Full Length Article

The adsorption of CO, O_2 and H_2 on Li–doped defective (8,0) SWCNT: A DFT study

C.R. Luna*, P. Bechthold, G. Brizuela, A. Juan*, C. Pistonesi

Departamento de Física and Instituto de Física del Sur (UNS–CONICET), Av. Alem 1253, 8000 Bahía Blanca, Argentina

A B S T R A C T

This work presents a theoretical study, based on DFT calculations, about the changes induced when diatomic molecules (CO, O_2 and H_2) are adsorbed on defective (8,0) SWCNT doped with a Li atom. The adsorption of one Lithium atom is tested inside and outside of the nanotube containing a single vacancy. The Li atom induces a magnetic moment on the nanotube and an important reduction in its the band gap (E_g). The adsorption energy values (E_{ads}) for CO, O_2 and H_2 when Li is located inside, are higher than when Li is outside. The H_2 adsorption does not change the magnetic nature of the system. However, the CO and O_2 molecules reduce the magnetic moment from 1.0 μ_B to 0.0 μ_B. The band gap energy is reduced for CO and O_2, while increases in the case of H adsorption. The work function (WF) value is reduced in the cases of CO and H_2; whereas for O_2 we observed an opposite behavior, then the final charge state of this molecule is negative. Based on our results, the system Li + defective (8,0) SWCNT can be proposed as possible candidate as gas sensor of CO,O_2 and H_2.

1. Introduction

The use of gas sensors as monitoring devices has become crucial for industrial, environmental and medical processes [1]. Carbon nanotubes (CNTs) have shown a great potential to be used as gas sensors, they have more active adsorption sites than other materials. This is attributable to their high curvature and the fact that almost all its surface is exposed to the environment [1–4]. Particularly, semiconducting single walled carbon nanotubes (SWCNTs) have demonstrated that their conductivity change rapidly when gas is adsorbed [2,5–8]. In addition, the gas adsorption is improved when the SWCNTs are decorated with impurities (e.g. transition metal or alkali metal) and/or there are defects in their structure [9–17]. Nevertheless the transition metal atoms tend to form clusters on the nanotube, due to their high cohesive energy [19–22]. The cluster formation decreases metal dispersion while increases metal-metal interaction, reducing gas adsorption. For example Sun et. al. [22] found that Ti atoms prefer to form clusters on the C_{60} surface. Similar results are reported on SWCNT with Rh [18,19]. On the other hand, a theoretical study reports that doping carbon fullerenes with alkali atoms (Li, Na and K) improves the molecular hydrogen adsorption capacity of them [23]. Authors conclude that the effect is more evident for sodium and lithium. The experimental work performed by Goudarziet. al. found that Li doped SWCNTs improve the adsorption NH_3 gas [2]. In addition, the detection of poisonous gas SO_2 using SWCNTs is actually very studied by the scientific community [24–26]. For example, Yoosefian and co–workers by using DFT calculations investigated the adsorption of single and double SO_2 gas molecule(s) on the surface of Pt–doped and Au–doped (5,5) SWCNTs with a single vacancy [25]. Their results show that the adsorption energy of SO_2 is similar for both doping (Pt/Au); nevertheless the change in the energy gap value is more significant when the molecule is adsorbed on Pt/SWCNT. Li et al. study theoretically the adsorption of the same molecule on Ni–doped vacancy–defected (8,0) SWCNT [26]. The authors conclude that the vacancy improves the SO_2 adsorption. Moreover, after the Ni doped on the vacancy of the SWCNT, the modified nanotube which were not very much sensitivity to SO_2 molecule could become much sensitivity to it. The (8,0) SWCNT has been studied extensively and presents interesting physical and chemical properties because it is one of the smallest diameter semiconductor carbon nanotube [27–29]. These studies reveal a significant modification in the electronic configuration of the CNT after the adsorption of CO, O_2 and H_2 molecules. In addition, the adsorption of H, H_2, and/or TM atoms (particularly TMs with unfilled d orbitals) on SWCNTs can create an active site and induce magnetism in the CNT, making the impurity–SWCNT a potential system for both hydrogen storage and spintronics applications.

There are a few studies about the interaction between Li and single walled carbon nanotube containing a single vacancy; but to the best of our knowledge there are still no investigations about its possible role as a sensor of diatomic molecules [30,31]. For this reason, the aim of this work is to analyze the Li doped defective (8,0) SWCNT as a possible candidate for a gas sensor development. The changes on its physical properties when it interacts with the more common diatomic gases usually sensed in industrial processes, such as CO, H_2 and O_2 are

* Corresponding author at: Departamento de Física and Instituto de Física del Sur (UNS–CONICET), Av. Alem 1253, 8000 Bahía Blanca, Argentina.
E-mail address: cluna@uns.edu.ar (C.R. Luna).

https://doi.org/10.1016/j.apsusc.2018.07.171
Received 4 April 2018; Received in revised form 17 June 2018; Accepted 24 July 2018
Available online 30 July 2018
0169-4332/

studied using Density Functional Theory (DFT) calculations.

2. Computational model

First principles calculations based on Density Functional Theory (DFT) implemented through the Vienna Ab initio Simulation Package (VASP) code are used [32,33]. The exchange-correlation functional corresponds to the generalized gradient approximation (GGA) and the Perdew, Burke, and Ernzerhof (PBE) functional were considered [34,35] with a plane–wave basis set, implementing the projector–-augmented–wave (PAW) method developed by Kresse [32]. The kinetic energy cutoff of 700 eV is found to converge the total energy within 10^{-4} meV. In addition, Brillouin zone sampling is performed using the k–point generation scheme of Monkhorst and Pack (the Γ–point was included) [36]. For ionic relaxation calculations, the Brillouin zone is sampled by a k–point mesh of 1 × 5 × 1 and the convergence criteria is set to be 10^{-3} eV/Å on each atom. We have included dispersion forces, as suggested in the literature [37,38], using the DFT–D2 Grimme method [39]. The conjugate gradient (CG) algorithm is used to find the minima of the total energy. Finally in order to compute the adsorption energies, magnetic moment, density of states (DOS) curves, Bader charges [40] and electrostatic potentials, the k–point mesh is increased from 5 to 21 k–points.

The (8,0) SWCNT is modeled using 64C atoms, where they are in a periodic supercell of 20 Å × 8.53 Å × 20 Å. This supercell size ensures no interaction among periodic images. For simulate the vacancy one C atom is removed, a detailed description of this defective nanotube was reported on our previous work [18].

The adsorption energy E_{ads} of a Li atom and an X molecule (X: CO, O_2 or H_2) are computed as:

$$E_{ads} = E_T(host + Li) - E_T(host) - E(Li) \quad (1)$$

$$E_{ads} = E_T(host + X) - E_T(host) - E(X) \quad (2)$$

The host system in Eq. (1) corresponds to SWCNT with a single vacancy whereas in Eq. (2) corresponds to defective SWCNT with a Li atom adsorbed. The E_T(host + Li) and E_T(host + X) are the total energies of the corresponding host system with the Li atom or X molecule adsorbed. E_T(host) is the energy of clean host system. The E(Li) and E(X) are the energies of one Li atom and isolated X molecule respectively. Finally, the work function (WF) is calculated as the vacuum energy level minus the Fermi level.

3. Results and discussion

3.1. Li adsorption on defective SWCNT

We found that the Li incorporation on a defective nanotube is energetically more favorable than on a pristine nanotube. For a Li atom located in an outer (inner) position, the adsorption energy in the SWCNT containing a single vacancy is 1.65 eV (1.75 eV) stronger than in the pristine nanotube. The structure of (8,0) SWCNT containing a single carbon vacancy and a Li atom adsorbed is fully relaxed. The Li adsorption is considered both outside and inside of the defective nanotube; in both cases several adsorption sites for Li are tested. Fig. 1 shows the optimized structures for the most energetically stable sites. It can be noted that there is a modification in the SWCNT curvature due to the Li adsorption, which is more pronounced for the outer adsorption case. The distance between opposite atoms in the nanotube increases from 6.67 Å to 6.98 Å (6.82 Å) in the Li–vacancy direction, for outside (inside) adsorption; whereas in the perpendicular Li–vacancy direction, the distance is almost the same (5.99 Å).

Almost all the C—C bond distances remain unchanged after Li adsorption only the longest C—C bond of 1.82 Å is modified, from 1.82 Å to 1.52 Å (see Fig. 1). In the case of outer adsorption, the Li atom is bonded to three C atoms, named C1, C2 and C3 (see Fig. 1b). The Li—C bond distances are 2.11 Å, 2.21 Å and 2.24 Å respectively. For the internal adsorption case, the Li atom is bonded to two C atoms (C4 and C5) with bond distances of 2.23 Å and 2.24 Å respectively (see Fig. 1c). Similar values were reported by Udomvech et al. [41].

Table 1 shows the computed band gap (E_g), magnetic moment (μ) and work function (WF) for the defective SWCNT. Li adsorption energy (E_{ads}) is also included for Li doped systems. The defective (8,0) SWCNT is a semiconductor with a computed band gap of 0.48 eV [18]. The alkali metal incorporation reduces the band gap in both cases; 81% for Li outer and 50% for Li inner. The defective nanotube has no magnetic moment, but the Li adsorption induces a magnetic moment of 1.0 μ_B, independently of the Li atom location. The work function is reduced about a 22% (from 4.89 eV to 3.82 eV) and 10% (from 4.89 eV to 4.39 eV) for outside and inside Li adsorption respectively. The reduction in the WF implies that there is an electron transfer from the Li atom to the nanotube, further discussion about this behaviour is explained below. The Li adsorption energy (E_{ads}) for outer side is 0.33 eV energetically more favorable than for the inside location which is in agreement with literature results [42].

The total density of states (TDOS) and projected density of states (PDOS) for Li + (8,0) SWCNT, with both adsorption configuration, are shown in Fig. 2. The dotted line indicates the Fermi level and spin up and spin down contributions are shown. From PDOS curves it can be noted that the C atoms contribute more than Li to the valence band (VB), but both elements contribute almost equally to the conduction band (CB). The Li induces states in the band gap zone due to its hybridization with C atoms, this fact leads to a half–metallic behaviour of the Li + nanotube system, as can be seen in Fig. 2. It is also noted from TDOS curves, that near the Fermi level is where the most notorious differences between spin up and down contributions are observed, and outside this zone both contributions are almost symmetrical. This behaviour of spin up and down contributions could be interesting in spintronic area.

From Bader charges analysis is noted that the Li atom transfers electrons to the carbon atoms located nearby it (see Fig. 3), that is to say the lithium becomes positively charged after adsorption. This fact agrees with the WF reductions after Li adsorption reported in Table 1. The Li atom loses 0.89 e^- and 0.91 e^- for outer and inner locations respectively. As a result, the (8,0) SWCNT becomes negatively charged and this behaviour makes it a good candidate to be used as a negative electrode in Lithium –ion batteries, as was already reported by several authors [42–45]. It can be noted that the major transfer to C atoms (0.33 e^-) occurs in the case of Li located outside, this can be attributed to the fact that Li is closer to the nanotube.

3.2. Gas adsorption

The adsorption of the diatomic molecules, CO, O_2 and H_2 on Li + (8,0) SWCNT is studied at several adsorption sites and orientations. We report here only the most stable configurations. The computed band gap (E_g), magnetic moment (μ), work function (WF) and adsorption energy (E_{ads}) values are listed in Table 2. For outer Li configuration, the CO (H2) adsorption increases the band gap E_g value from 0.09 eV to 0.22 eV (0.21 eV) (compare Tables 1 and 2); whereas the O_2 adsorption reduces de band gap from 0.09 eV to 0.00 eV, this behavior is discussed later. When the Li atom is located inside the nanotube, H_2 adsorption increases the band gap from 0.24 eV to 0.33 eV, while CO and O_2 adsorption reduces E_g, again to a null value for the case of the oxygen molecule, as can be seen in Table 2.

On the other hand, CO and H_2 molecules adsorption do not modify the magnetic moment of the system when the Li atom is located outside. But the O_2 molecule leads to an increase of the magnetic moment value, from 1.0 μ_B to 2.0 μ_B. In the case of gas adsorption for the inner Li configuration, the CO and O_2 reduce the magnetic moment from 1.0 μ_B to 0.0 μ_B, while the H_2 adsorption does not modify the magnetic moment value (see Table 2).

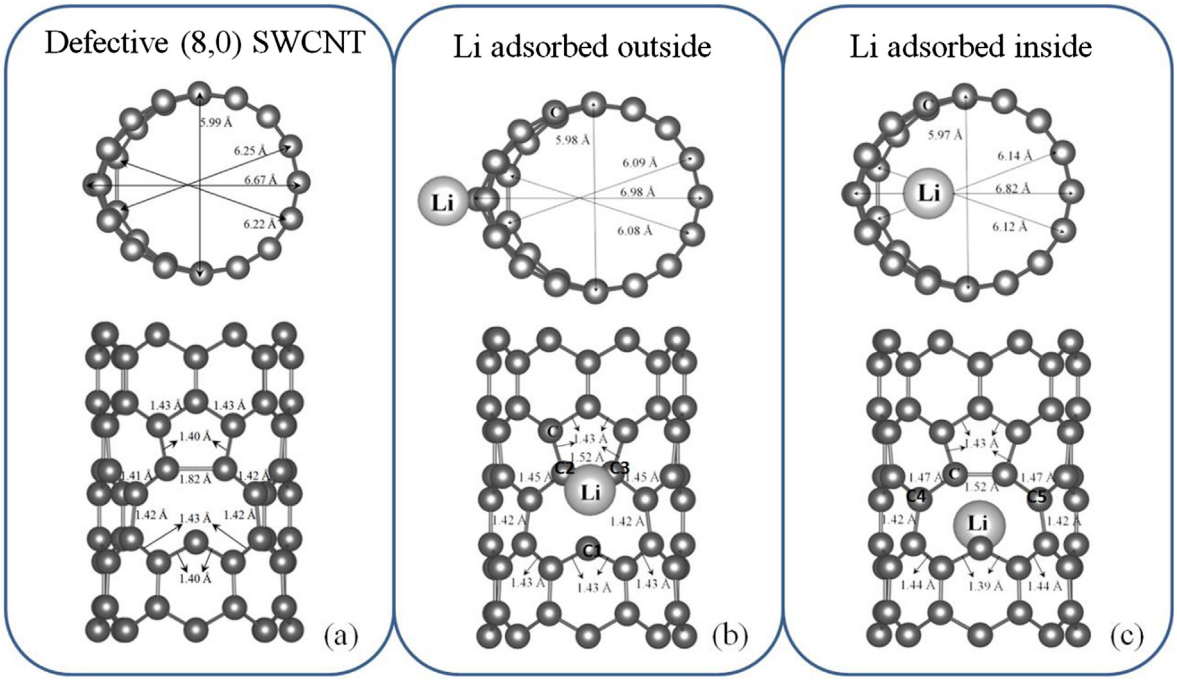

Fig. 1. Optimized atomic structures of (8,0) SWCNT: (a) containing a reconstructed single vacancy and a Li atom adsorbed (b) outside and (c) inside.

Table 1
Band gap (E_g), magnetic moment (μ), work function (WF) and adsorption Energy (E_{ads}) for defective (8,0) SWCNT and Li adsorbed outside and inside the nanotube.

	System		
	Defective SWCNT	Li outside	Li inside
E_g(eV)	0.48	0.09	0.24
μ(μ_B)	0.00	1.00	1.00
WF(eV)	4.89	3.82	4.39
E_{ads}(eV)	–	−3.21	−2.88

The CO, O_2 and H_2 adsorption on Li(out)+SWCNT induces an increase in the WF value of a 5%, 25% and 5%, respectively, with respect to the clean Li (out)+SWCNT. Comparing Tables 1 and 2 it can be noted that the WF increases 1% when O_2 is adsorbed on the inner Li configuration and the WF decreases 8% (1%) after CO (H2) adsorption.

From Table 2, it can be noted that O_2 adsorption has the highest E_{ads} value with respect to the other molecules, for Li outside E_{ads} is −0.84 eV and for Li inside its value is −5.66 eV. This behaviour can be attributed to the fact that the vacancies generally are in a oxygenated state [10]. It is also observed that E_{ads} values for CO, O_2 and H_2 on Li (in)+(8,0) SWCNT are 3.5 eV, 4.8 eV and 1.6 eV higher than the ones obtained in Li(out)+(8,0) SWCNT, respectively, (see Table 2). So gas adsorption is much more favorable when the Li is located inside the nanotube. This could be attributed to the fact that the molecules can interact more directly with the vacancy defect on the SWCNT. Next we will analyse these cases in detail.

The optimized structures of CO, O_2 and H_2 adsorbed on Li(in) +SWCNT are shown in Fig. 4. Li + SWCNT takes a role in the initial steps for the O_2 and H_2 dissociation. After optimization the O—O bond length varies from 1.48 Å to 2.58 Å , whereas in the case of H_2 adsorption the H—H bond is elongated from 0.75 Å to 1.70 Å. The opposite effect is observed for the CO molecule, in which its bond length is reduced from 1.46 Å to 1.39 Å. In all cases the adsorbates affect mainly the longest C—C bond of the SWCNT. Comparing the Fig. 1c and Fig. 4, it is observed that this C—C bond increases its value from 1.52 Å to 2.83 Å, 2.31 Å and 2.70 Å after CO, O_2 and H_2 adsorption, respectively. The other C—C bond lengths remain almost unchanged.

In the case of CO adsorption, a C—O—C ether group is formed. The carbon atom of CO molecule, named C^*, is adsorbed on the center of the vacancy and the O atom is located above the nanotube between two C atoms, C^* and C1 in Fig. 4a. The results obtained show that both C—O bond lengths are 1.39 Å and the C—O—C angle is 94°, the remaining C—C—O angles are 43° (see Fig. 4a). In addition, after O_2 adsorption on the Li (in)+SWCNT two functional groups are formed, a C—O—C (ether) and a C═O (ketone). For the ether group both C—O bond distances are 1.46 Å (O bonded to C1 and C2, see lower part of Fig. 4b), whereas for the ketone group the C—O bond length is 1.22 Å (O bonded to C3, see upper part of Fig. 4b). These results are in agreement with experimental findings indicating the presence of oxygenated vacancies in carbon nanotubes [19,46]. For H_2 adsorption is noted the development of two C—H hydrocarbons, named C1—H and C2—H in Fig. 4c. The bond lengths obtained are the same for both hydrocarbons and they are about 1.08 Å.

In all cases the gas molecule adsorption induces a deformation in the nanotube curvature, as can be seen in Fig. 4. The diameter elongation is major when O_2 interacts with the nanotube, incrementing from 6.82 Å to 7.38 Å (compare Fig. 1c and Fig. 4b). Then it is expected that these curvature changes lead to electronic modifications.

In order to investigate the electronic properties after molecule interactions with Li + SWCNT, we have calculated the density of states (DOS) corresponding to CO, O_2 and H_2 adsorbed on Li (in)+(8,0) SWCNT. Fig. 5 shows the total and projected density of states (PDOS). The Li(in)+SWCNT is a semiconductor, with a band gap of 0.24 eV. When the molecule is adsorbed the band gap value is modified depending on the adsorbed molecule (see Table 2). In the case of CO and O_2 there is a band gap reduction. This fact can be attributed to the presence of new states at the Fermi level region as shown in Fig. 5a–b. Specifically in the case of O_2 adsorption, the band gap value reduces to zero, thus the system shows a metallic, instead of a semiconductor behavior. Due to this sensibility to the band gap value, the Li(in) +SWCNT could be considered a potential candidate to be used as CO and O_2 gas sensor. In the case of hydrogen adsorption, there is an increases of band gap value and this fact is shown in Fig. 5c.

Regarding the CNT C atoms, from Fig. 5d–f is observed that their contributions to the TDOS curve are both in the valence (VB) and the

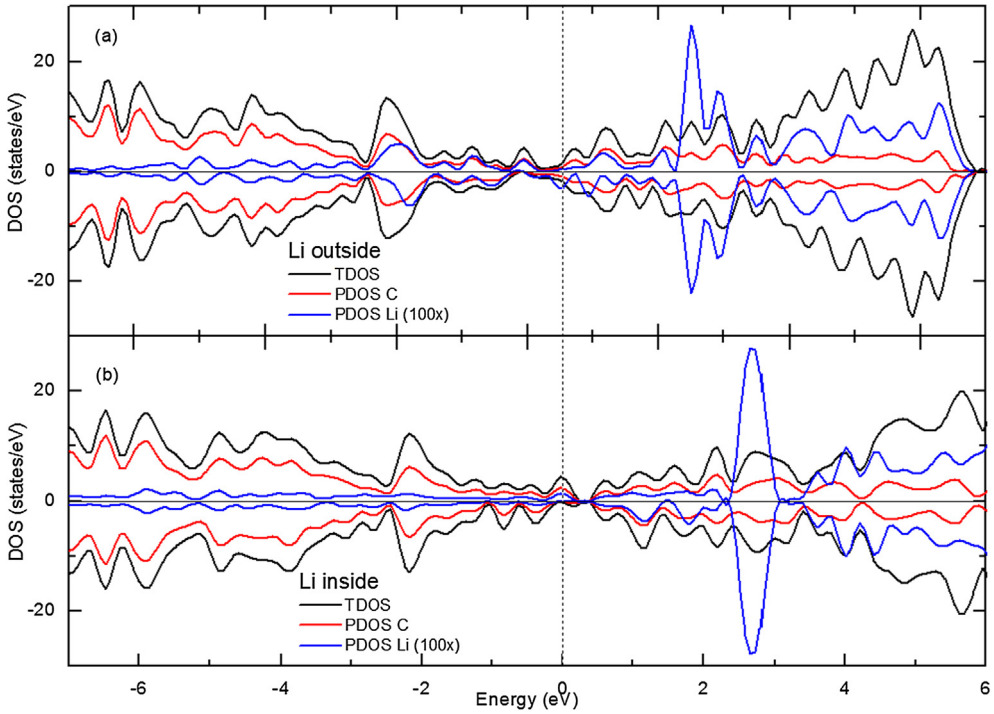

Fig. 2. Density of states for Li adsorption on defective (8,0) SWCNT. Total and Projected DOS curve for Li adsorbed (a) outside and (b) inside of the nanotube. The dotted line indicates the Fermi level.

conduction band (CB). The Li contribution is mainly at the CB. In addition to this, if we compare these Figs with Fig. 2b, it is noticed that the interaction between the Li atom and the SWCNT has no significant changes after gas adsorption. The PDOS curves for each molecule before and after adsorption are present in Fig. 5g–i. The localized states of the isolated molecule are clearly modified after adsorption. This fact is due to hybridization between the diatomic molecule and the adsorbate (Li + SWCNT). In all cases main peaks are shifted towards lower energy values, resulting on a stabilization of the system.

Particularly, for CO adsorption it can be noted that the Fermi level is shifted to higher energy values with respect to Li + SWCNT. This fact

Table 2
Band gap (E_g), magnetic moment (μ), work function (WF) and adsorption Energy (E_{ads}), for CO, O_2 and H_2 adsorbed on Li + (8,0)SWCNT, with Li located outside and inside the nanotube.

	Li outside			Li inside		
	CO	O_2	H_2	CO	O_2	H_2
E_g (eV)	0.22	0.00	0.21	0.12	0.00	0.33
μ (μ_B)	1.00	2.00	1.00	0.00	0.00	1.00
WF (eV)	4.01	4.79	4.02	4.03	4.43	4.35
E_{ads} (eV)	−0.44	−0.84	−0.25	−3.94	−5.66	−1.88

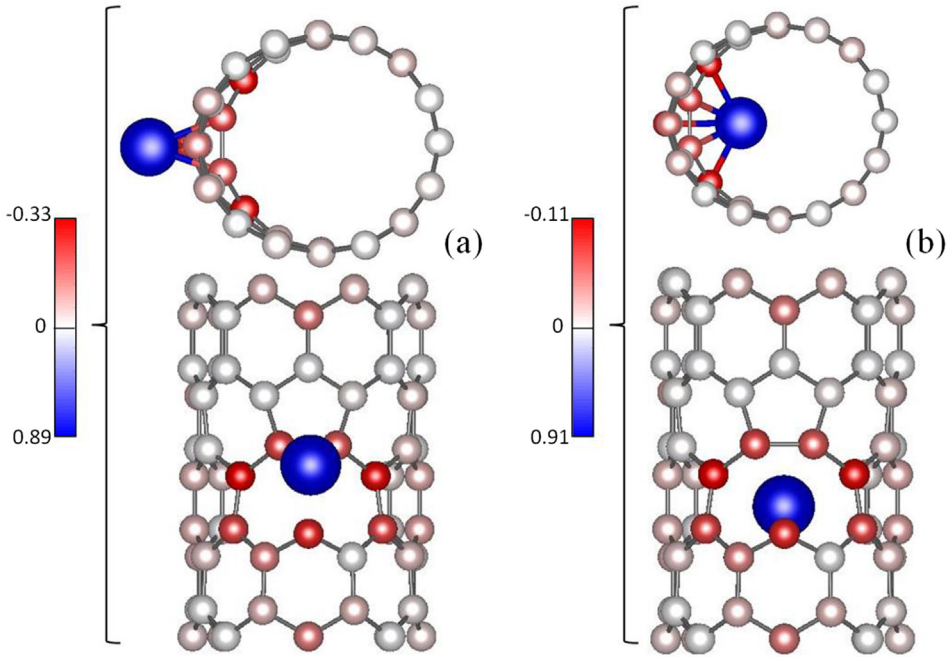

Fig. 3. Charge transfer between Li and C atoms of the SWCNT containing a single vacancy. Li adsorbed (a) outside and (b) inside in defective SWCNT. Red and blue indicate that the atom gains (negative charge) and loses electrons (positive charge) respectively. The bar on the left is in e^- unit. (For interpretation of the references to colour in this figure legend, the reader is referred to the web version of this article.)

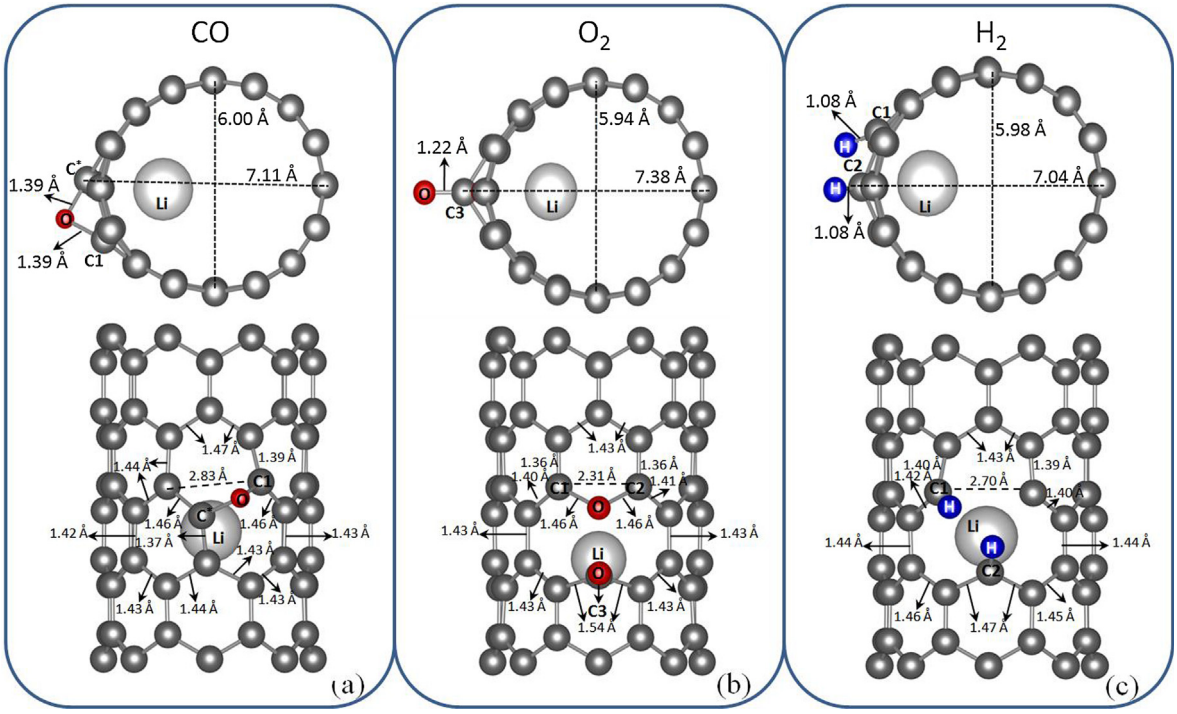

Fig. 4. Optimized atomic structures for adsorption of some molecules on (8,0) SWCNT containing a reconstructed single vacancy and with a Li atom adsorbed inside. (a) CO, (b) O_2 and (c) H_2. The C^* atom corresponds to the carbon atom of the CO molecule.

attributes the n–type semiconductor nature when CO is adsorbed on Li + SWCNT. Spin up and spin down contributions are symmetric for energy values below 4 eV; this fact is in accordance with the almost null magnetic moment of the system. The peak located around −5 eV comes mainly from the hybridization between the O atom of CO molecule and the SWCNT, as can be seen in Fig. 5d and g.

The O_2 interaction with Li doped SWCNT is different than in the case of CO or H_2 adsorption. As we have mentioned before, new states are generated in the band gap region. This fact arises a metallic behavior for the Li(in) + SWCN + O_2 system. Then we can expect optical features [47]. The Li and C PDOS curves show an increase on the peak intensities for energy values higher than 4 eV (see Fig. 5e), due to the O_2 molecule presence. Again, TDOS curves are almost symmetrical below 4 eV, reflecting the non magnetic behavior of the system.

Regarding the H_2 adsorption, we obtain the highest band gap value (0.33 eV) as is well noted in Fig. 5c. On the other hand the magnetic moment is 1.00 μ_B, this is in accordance with the asymmetrical behaviour of TDOS curves. The Fermi level is located nearer to VB than CB, so the H_2 adsorption on Li + SWCNT has a p–type semiconductor behaviour. The interaction of the dissociated hydrogen molecule is mainly with states of the SWCNT carbon atoms in the valence band zone, below −3 eV, see Fig. 5f and i. The magnetic and semiconductor nature of this system could have interesting applications in permanent magnetism, magnetic recording, and spintronics, besides as a gas sensor.

The charge transfer between the adsorbed species and the adsorbate are presented in Fig. 6. In all cases the Li atom loses electrons becoming positively charged. The carbon atoms of the nanotube, closer to the adsorbed species are also positively charged in the cases of CO and O_2 adsorption, whereas for H_2 these C atoms gain electrons. The major electron transfer occurs in the case of the dissociated O_2 molecule, as can be seen in Fig. 6.

Table 3 shows the number of electrons of each studied specie before and after adsorption. Specifically for the CO molecule, which adsorbs on the surface, electronic populations and charge for the whole molecule are indicated on Table 3. For O_2 and H_2, which dissociate on the surface, individual atomic populations and charges are reported. Before adsorption the molecule state is electrically neutral; whereas, after adsorption the electron density is modified due to the interaction with the host system Li(in) + SWCNT. The CO molecule and the H atoms (from H_2 molecule) have a positive charge state after adsorption, in agreement with the WF function reductions. An opposite behaviour is obtained for the oxygen atoms (from O_2 molecule), presenting a negative charged state, also in agreement with a WF increases (see Table 2). CO and dissociated H_2 molecule lose a small amount of charge (about of 0.1 e^-) whereas both O atoms (from O_2 molecule) gain about 3.4 e^-.

4. Conclusion

The (8,0) SWCNT with a single vacancy is more favorable for the adsorption of one Li atom than pristine (8,0) SWCNT. From adsorption energy (E_{ads}) calculations we can conclude that on defective SWCNT the Li location could be inside or outside the nanotube. From the results is noted that the presence of Lithium induces a magnetic moment of 1.0 μ_B and a reduction of band gap value from 0.48 eV to 0.09 eV and 0.24 eV for outer and inner Li, respectively. The Li atom acts as a donor of electrons, that is to say the defective nanotube after adsorption is negatively charged. These facts make the system Li + (8,0) SWCNT a good candidate to be used as a negative electrode in Lithium–ion batteries and to be used in spintronic area.

The CO, O_2 and H_2 molecules were adsorbed on Li + defective(8,0) SWCNT. The adsorption energy values for each molecule corresponding to both Li locations, show that adsorption is energetically more favorable when the Li atom is located on the inner side of the nanotube. This could be attributed to the fact that the diatomic molecule interacts directly with the vacancy. The band gap, magnetic moment and work function values are modified after CO, O_2 and H_2 adsorption. In addition, the SWCNT curvature and bond lengths of the molecule, nanotube C–C, and Li–C distances are also altered due after adsorption.

The host system Li(in) + (8,0)SWCNT dissociates the O_2 and H_2 molecules, whereas the CO molecule reduces its bond distance. In each case new functional groups are formed, as ether, ketone or

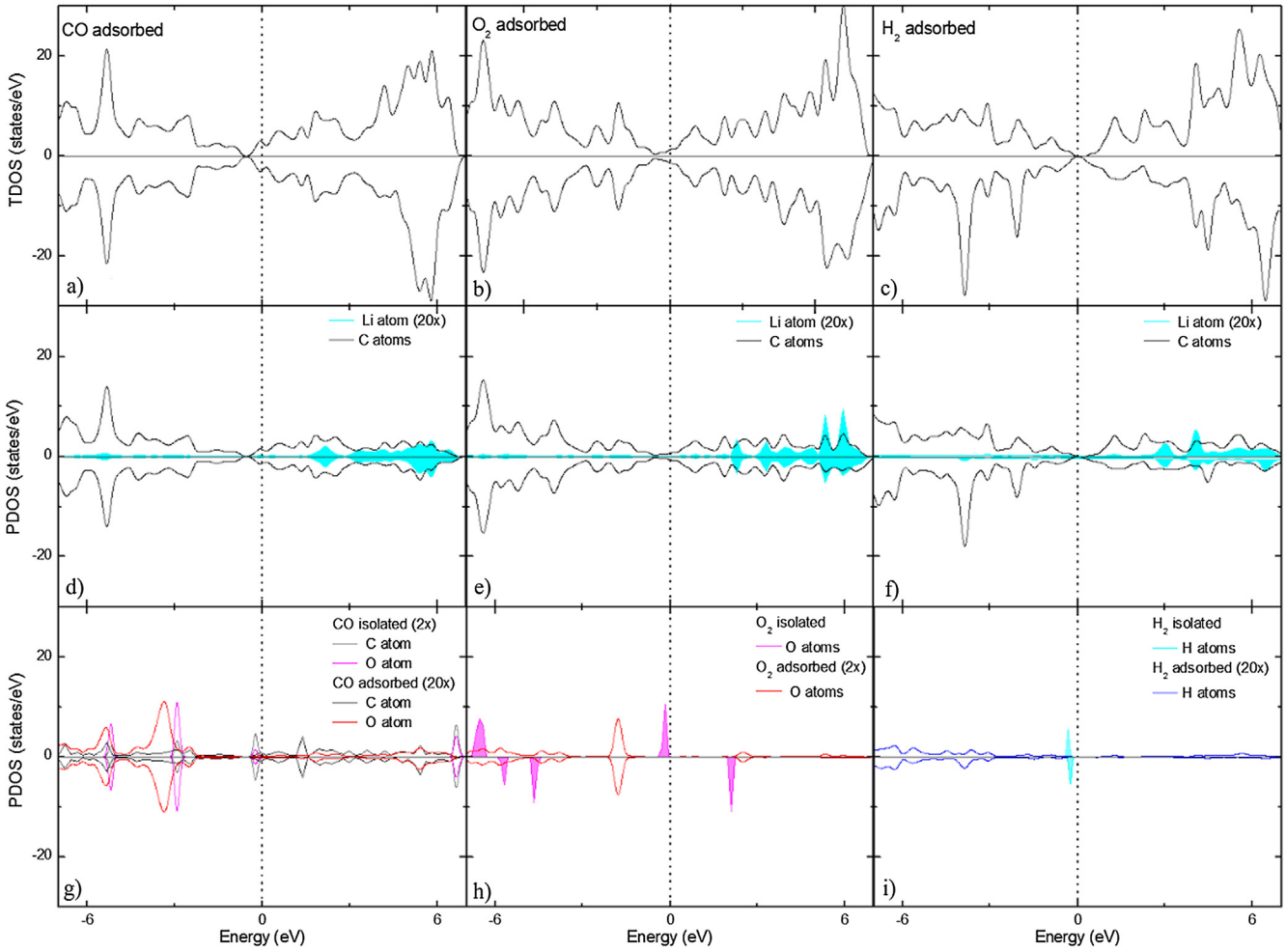

Fig. 5. Total and projected density of states, TDOS and PDOS, for the CO, O_2 and H_2 molecules adsorbed above Li + (8,0) SWCNT vacancy. The Li is located inner in the nanotube. The dotted line indicates the Fermi level.

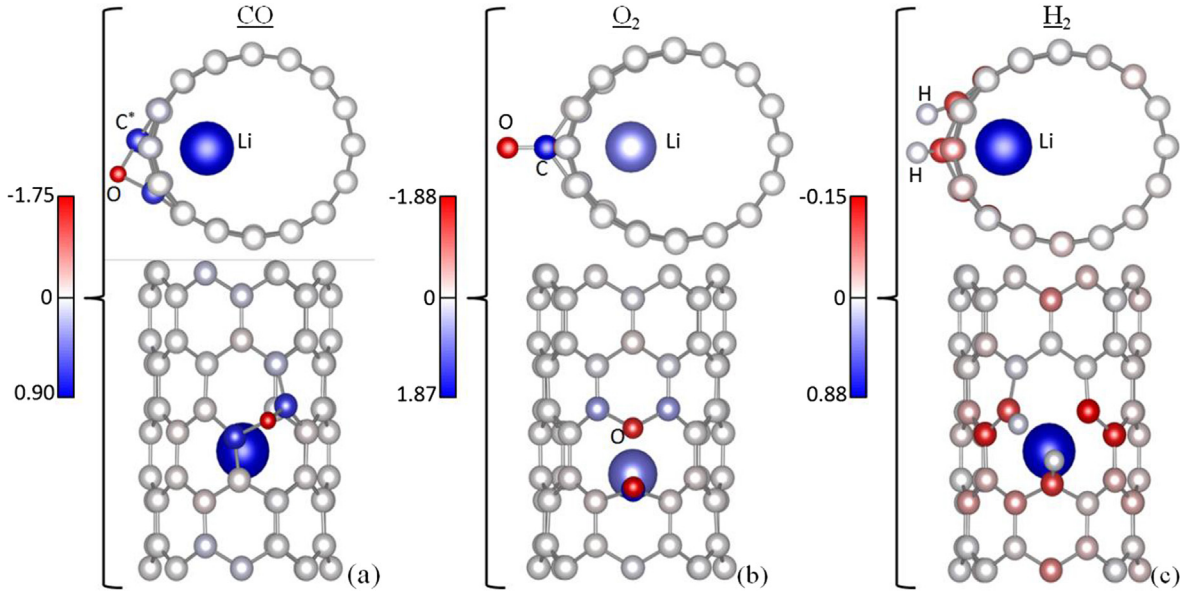

Fig. 6. Charge transfer between the adsorbed species (CO, O_2 or H_2), Li and C atoms of the SWCNT with a single vacancy. (a) CO, (b) O_2 and (c) H_2. Red and blue indicate that the atom gains (negative charge state) and loses (positive charge state) electrons respectively. The bar on the left is in e^- unit.

Table 3
Changes in electronic population for each molecule/atom before and after adsorption on Li(in) + SWCNT. The Δ column represents the net charge of each specie after adsorption. These columns are in e^- units. The last corresponds to the final charge state of each adsorbed specie on Li + SWCNT.

Specie	Before adsorption (e^-)	After adsorption (e^-)	Δ	Charge state
CO	10	9.84	0.16	Positive
O1	6	7.52	−1.52	Negative
O2	6	7.88	−1.88	
H1	1	0.96	0.04	Positive
H2	1	0.93	0.07	

*O1 and O2 correspond to the oxygen atoms of ether and ketone group respectively.

hydrocarbons. Based in our results we can conclude that defective Li + (8,0) SWCNT is a potential candidate to be used as gas sensor of CO, O_2 and H_2 due to the changes on its physical properties during adsorption. Specifically after CO adsorption, Li(in) + (8,0)SWCNT changes from magnetic to non magnetic and reduces its band gap. More changes are produced due to O_2 interaction: the system becomes non magnetic and it shows a metallic instead of a semiconductor behavior. Finally due to H_2 interaction with the system an increment on the band gap energy is observed.

Acknowledgements

We acknowledge the financial support given by SGCyT–UNS, CONICET–PIP 2014–2016:GI11220130100436CO, PIP 2015–2017 11220150100456CO, PICT 2014–1351, 2012–2186 and 2016–4085. All authors are members of CONICET.

References

[1] W. An, X. Wu, X.C. Zeng, Adsorption of O_2, H_2, CO, NH_3, and NO_2 on ZnO nanotube: a density functional theory study, J. Phys. Chem. C 112 (2008) 5747–5755.
[2] F. Goudarzi, M.R. Vaezi, A. Kazemzadeh, Ceramic processing research a novel single wall carbon nanotubes-based sensor doped with lithium for ammonia gas detection, J. Ceram. Process. Res. 13 (2012) 612–616.
[3] B.S. Dasari, W.R. Taube, P.B. Agarwal, Room temperature single walled carbon nanotubes (SWCNT) chemiresistive ammonia gas sensor, Sens. Transd. 190 (2015) 24–30.
[4] N.L.W. Septiani, B. Yuliarto, Review—the development of gas sensor based on carbon nanotubes, J. Electrochem. Soc. 163 (2016) 97–106.
[5] S. Fan, Self-oriented regular arrays of carbon nanotubes and their field emission properties, Science 283 (1999) 512–514.
[6] P. Bondavalli, P. Legagneux, D. Pribat, Carbon nanotubes based transistors as gas sensors: state of the art and critical review, Sens. Actuat. B Chem. 140 (2009) 304–318.
[7] C. Cantalini, L. Valentini, I. Armentano, J.M. Kenny, L. Lozzi, S. Santucci, Carbon nanotubes as new materials for gas sensing applications, J. Eur. Ceram. Soc. 24 (2004) 1405–1408.
[8] J.-M. Tulliani, A. Cavalieri, S. Musso, E. Sardella, F. Geobaldo, Room temperature ammonia sensors based on zinc oxide and functionalized graphite and multi-walled carbon nanotubes, Sens. Actuat. B Chem. 152 (2011) 144–154.
[9] M. Yoosefian, A high efficient nanostructured filter based on functionalized carbon nanotube to reduce the tobacco-specific nitrosamines, NNK, Appl. Surf. Sci. 434 (2018) 134–141.
[10] M. Yoose, N. Etminan, RSC advances properties, stability and reactivity trend of a tryptophane/Pd doped SWCNT novel nanobiosensor from polar protic to non-polar, RSC Adv. 6 (2016) 64818–64825.
[11] X. Peng, S.A. Meguid, Molecular dynamics simulations of the buckling behavior of defective carbon nanotubes embedded in epoxy nanocomposites, Eur. Polym. J. 93 (2017) 246–258.
[12] N. Etminan, M. Yoose, H. Raissi, M. Hakimi, Solvent effects on the stability and the electronic properties of histidine/Pd-doped single-walled carbon nanotube biosensor, J. Mol. Liq. 214 (2016) 313–318.
[13] M. Yoosefian, Applied surface science powerful greenhouse gas nitrous oxide adsorption onto intrinsic and Pd doped Single walled carbon nanotube, Appl. Surf. Sci. 392 (2017) 225–230.
[14] Y. Yang, C. Ramirez, X. Wang, Z. Guo, A. Tokranov, R. Zhao, I. Szlufarska, J. Lou, B.W. Sheldon, Impact of carbon nanotube defects on fracture mechanisms in ceramic nanocomposites, Carbon 115 (2017) 402–408.
[15] M. Yoosefian, A. Pakpour, N. Etminan, Applied surface science nanofilter platform based on functionalized carbon nanotubes for adsorption and elimination of acrolein, a toxicant in cigarette smoke, Appl. Surf. Sci. 444 (2018) 598–603.
[16] M. Yoosefian, N. Etminan, Leucine/Pd–loaded (5,5) single–walled carbon nanotube matrix as a novel nanobiosensors for in silico detection of protein, Amino Acids 50 (2018) 653–661.
[17] J.A. Robinson, E.S. Snow, C. Ba, T.L. Reinecke, F.K. Perkins, Role of defects in single-walled carbon nanotube chemical sensors, Nano Lett. 6 (2006) 1747–1751.
[18] R. Ambrusi, C.R. Luna, M.G. Sandoval, P. Bechthold, M.E. Pronsato, A. Juan, Rhodium clustering process on defective (8,0) SWCNT: analysis of chemical and physical properties using density functional theory, Appl. Surf. Sci. 425 (2017) 823–832.
[19] I. Suarez-Martinez, C.P. Ewels, X. Ke, G. Van Tendeloo, S. Thiess, W. Drube, A. Felten, J.-J. Pireaux, J. Ghijsen, C. Bittencourt, Study of the interface between Rhodium and carbon nanotubes, ACS Nano 4 (2010) 1680–1686.
[20] Y. Shibuta, S. Maruyama, Bond-order potential for transition metal carbide cluster for the growth simulation of a single-walled carbon nanotube, Comput. Mater. Sci. 39 (2007) 842–848.
[21] X. Wu, X.C. Zeng, Adsorption of transition-metal atoms on boron nitride nanotube: a density-functional study, J. Chem. Phys. 125 (2006) 44711.
[22] Q. Sun, Q. Wang, P. Jena, Y. Kawazoe, Clustering of Ti on a C_{60} surface and its effect on hydrogen storage, J. Am. Chem. Soc. 127 (2005) 14582–14583.
[23] K.R.S. Chandrakumar, S.K. Ghosh, Alkali-metal-induced enhancement of hydrogen adsorption in C_{60} fullerene: an ab initio study, Nano Lett. 8 (2008) 13–19.
[24] X. Zhang, H. Cui, X. Dong, D. Chen, J. Tang, Adsorption performance of Rh decorated SWCNT upon SF_6 decomposed components based on DFT method, Appl. Surf. Sci. 420 (2017) 825–832.
[25] M. Yoosefian, M. Zahedi, A. Mola, S.A. Naserian, DFT comparative study of single and double SO_2 adsorption on Pt-doped and Au-doped single-walled carbon nanotube, Appl. Surf. Sci. 349 (2015) 864–869.
[26] W. Li, X.-M. Lu, G.-Q. Li, J.-J. Ma, P.-Y. Zeng, J.-F. Chen, Z.-L. Pan, Q.-Y. He, First-principle study of SO_2 molecule adsorption on Ni-doped vacancy-defected single-walled (8,0) carbon nanotubes, Appl. Surf. Sci. 364 (2016) 560–566.
[27] Z. Karami, S.J. Hashemifar, S.M. Sayedi, M.H. Sheikhi, First-principles study of H_2 adsorption on the pristine and oxidized (8,0) carbon nanotube, Int. J. Hydrogen Energ. 38 (2013) 13680–13686.
[28] J. Zhao, Y. Ding, Theoretical study of the interactions of carbon monoxide with Rh-decorated (8,0) single-walled carbon nanotubes, Mater. Chem. Phys. 110 (2008) 411–416.
[29] A. Star, V. Joshi, S. Skarupo, D. Thomas, J.P. Gabriel, V. Emery, Gas sensor array based on metal-decorated carbon nanotubes, J. Phys. Chem. B 110 (2006) 21014–21020.
[30] K.J. Li, Q.Y. Shao, J. Zhang, X.H. Yao, The stability and electronic structure of lithium adsorbed in triplet form of (5.0) carbon nanotubes and (5.0) boron nitrogen nanotubes: density functional theory studies, Mod. Phys. Lett. B 30 (2016) 1650220.
[31] S. Xu, Manipulation of separation selectivity for alkali metals using capped single-walled carbon nanotubes: a theoretical study, Appl. Mech. Mater. 687–691 (2014) 4307–4310.
[32] G. Kresse, D. Joubert, From ultrasoft pseudopotentials to the projector augmented-wave method, Phys. Rev. B 59 (1999) 1758–1775.
[33] G. Kresse, J. Hafner, Ab initio molecular dynamics for liquid metals, Phys. Rev. B 47 (1993) 558–561.
[34] J. Perdew, K. Burke, M. Ernzerhof, Generalized gradient approximation made simple, Phys. Rev. Lett. 77 (1996) 3865–3868.
[35] J.P. Perdew, K. Burke, M. Ernzerhof, Erratum: generalized gradient approximation made simple, Phys. Rev. Lett. 78 (1997) 1396.
[36] H.J. Monkhorst, J.D. Pack, Special points for brillouin-zone integrations, Phys. Rev. B 13 (1976) 5188–5192.
[37] R.E. Ambrusi, C.R. Luna, A. Juan, M.E. Pronsato, DFT study of Rh-decorated pristine B-doped and vacancy defected graphene for hydrogen adsorption, RSC Adv. 6 (2016) 83926–83941.
[38] Y.S. Al−Hamdani, D. Alfè, A. Michaelides, How strongly Do hydrogen and water molecules stick to carbon nanomaterials? J. Chem. Phys. 146 (2017) 94701.
[39] S. Grimme, Semiempirical GGA-type density functional constructed with a long-range dispersion correction, J. Comput. Chem. 27 (2006) 1787–1799.
[40] R.F.W. Bader, Atoms in Molecules, Encyclopedia of Computational Chemistry; John Wiley & Sons Ltd, Chichester, UK, 2002.
[41] A. Udomvech, T. Kerdcharoen, T. Osotchan, First principles study of Li and Li+ adsorbed on carbon nanotube: variation of tubule diameter and length, Chem. Phys. Lett. 406 (2005) 161–166.
[42] Z. Xiong, Y. Yun, H.-J. Jin, Applications of carbon nanotubes for lithium ion battery anodes, Mater. (Basel) 6 (2013) 1138–1158.
[43] M. Baibarac, M. Lira-Cantú, J. Oró-Solé, N. Casañ-Pastor, P. Gomez-Romero, Electrochemically functionalized carbon nanotubes and their application to rechargeable lithium batteries, Small 2 (2006) 1075–1082.
[44] P. Sehrawat, C. Julien, S.S. Islam, Carbon nanotubes in Li-ion batteries: a review, Mater. Sci. Eng. B 213 (2016) 12–40.
[45] J. Su, J. Zhao, L. Li, C. Zhang, C. Chen, T. Huang, A. Yu, Three-dimensional porous Si and SiO_2 with in situ decorated carbon nanotubes as anode materials for Li-Ion batteries, ACS Appl. Mater. Interf. 9 (2017) 17807–17813.
[46] K.A. Wepasnick, B.A. Smith, J.L. Bitter, D.H. Fairbrother, Chemical and structural characterization of carbon nanotube surfaces, Anal. Bioanal. Chem. 396 (2010) 1003–1014.
[47] V. Sgobba, D.M. Guldi, Carbon nanotubes—electronic/electrochemical properties and application for nanoelectronics and photonics, Chem. Soc. Rev. 38 (2009) 165–184.